

Chitosan coated chlorogenic acid and rutin composite phospholipid liposomes: Preparation, characterizations, permeability and pharmacokinetic

Cheng Zeng^{1,2}, Ruifang Zheng^{1,2}, Wen Jiang¹, Chenghui He²,
Jianguang Li^{1*} and Jianguo Xing^{2*}

¹College of Pharmacy, Xinjiang Medical University, Urumqi, Xinjiang, PR China,

²Xinjiang Institute of Materia Medica, Urumqi, Xinjiang, PR China

Abstract: In order to research and enhance bioavailability of chlorogenic acid and rutin(CA-R) via the oral route, chitosan coated composite phospholipid liposomes (C-CPLs) were applied to study on preparation, permeability and pharmacokinetic of C-CA-R-CPLs. The C-CA-R-CPLs were prepared by the method of ethanol injection. The entrapment efficiency (EE), average particle sizes, polymer disperse index (PDI), zeta potential, shape and *in vitro* drug release were investigated to characterize physicochemical parameters of C-CA-R-CPLs. The penetration properties from C-CA-R-CPLs were studied through Caco-2 cells model and the pharmacokinetics in Sprague-Dawley (SD) rats were evaluated by rat jugular vein intubation tube. The EE of C-CA-R-CPLs of CA and R was 91.3±2.13% and 92.6±2.44%, particle size of C-CA-R-CPLs was 176.7±2.3 nm, PDI was 0.207±0.014 and zeta potential of 12.61±1.33 mV. CA-R-CPLs and C-CA-R-CPLs were spherical or elliptical sphere and the bilayer of the CPL was observed obviously under transmission electron. The C_{max} , $t_{1/2}$ and $AUC_{0-12\text{h}}$ values of CA and R for groups of C-CA-R-CPLs were significantly increased. In conclusion, The C-CA-R-CPLs as a novel nano-formulation have potential to be used to enhance the oral bioavailability of poorly water-soluble drugs after oral administration.

Keywords: Chlorogenic acid, rutin, composite phospholipid liposome, chitosan, permeability, pharmacokinetic

INTRODUCTION

Saussurea involucrata (Traditional Chinese medicine, Uighur, Mongolian and Kazakhstan medicine), belongs to the Asteraceae family, is widely used for different therapeutic purposes in Xinjiang Uighur Autonomous Region of China (Xie *et al.*, 2017). Based on recent several studies, *Saussurea involucrata* is rich in phenylpropanoid and flavonoid content and has therapeutic effects on diabetes, hypercholesterolemia, fatty liver, hypertension and so forth (Liou *et al.*, 2017; Yao *et al.*, 2012).

Chlorogenic acid and rutin (CA and R, fig. 1) from the prepared *Saussurea involucrata* herba extract (SIHE), are two major active components and have a lot of significant biological activities, including anti-oxidant, anti-inflammatory and liver damage-resistant properties (Byambaragechaa *et al.*, 2014). Both CA and R are reported to play a significant role in hepatoprotective via improving liver oxidative stress resistance and inhibiting hepatic inflammatory (Su *et al.*, 2014). Thus, CA in combination with R could have obvious synergies effects to treat liver injury.

However, CA and R have low water solubility and poorly absorbed after oral administration (Chik *et al.*, 2015). In addition, they are unstable in the gastro-intestinal

environment and they were rapidly metabolized. These characteristics strongly influence absorption, cause low oral bioavailability (plasma concentration) and limit the effective applications and therapeutic efficacy of them. For these reasons, studies have been focused on means to improve their solubility in water and oral bioavailability.

In recent years, Composite phospholipid liposome (CPL) is an advanced nano-preparation delivery vehicle, which has been applied to pharmaceuticals to improve the biocompatibility, oral bioavailability of poorly water-soluble compounds, stability, cell membrane permeability and hepatic targetability, in addition, it has low toxicity (Vanić *et al.*, 2013; Klemetsrud *et al.*, 2016). According to several studies (Caddeo *et al.*, 2017; Zhou *et al.*, 2014; Tejera-Garcia *et al.*, 2014; Wang *et al.*, 2017), CPLs have smaller particle size, which can avoid reticuloendothelial system elimination and allow for a longer circulation plasma half-life. Besides, chitosan has hydrophilic, biocompatible, biodegradable and low toxicity (Huang *et al.*, 2014), which are able to resist the acid conditions of the stomach, interact with the gastrointestinal mucosa and promote the transport of macromolecules across epithelial tissue (Wieber *et al.*, 2011; Park *et al.*, 2014; Zeng *et al.*, 2017). Theoretically, it can enhance and promote the paracellular permeability of macromolecules and absorption of drug.

*Corresponding authors: e-mail: 442705861@qq.com, 925363296@qq.com

Up to now, neither permeability of Caco-2 cells nor in vivo investigations have not been reported by any studies on the effectiveness of CPL as a delivery system to enhance oral bioavailability of CA and R. Thus, for the first time, in this study, we have successfully prepared C-CA-R-CPLs to enhance drug delivery and compared to CA-R-solution and CA-R-CPLs in terms of transepithelial transport and oral bioavailability.

MATERIALS AND METHODS

Materials, chemicals and reagents

CA and R were obtained from Xinjiang Institute of Materia Medica (Xinjiang, China), purity 96%. Soybean Phospholipid (SPC, purity: 96%) were purchased from Lipoide Company (German). Lecithin Hydrogenated (HSPC, purity: 98%) were purchased from Shanghai Advanced Vehicle Technology Pharmaceutical Ltd., (Shanghai, China). Cholesterol were purchased from Hui Xing biochemical reagent Co. Ltd., (Shanghai, China). Chlorogenic acid (purity: 98%) and Rutin (purity: 98%) were purchased from National institutes for food and drug control (China). Sephadex G-50 were purchased from Beijing Pharmacia Company (China). Minimum essential medium (MEM) and fetal bovine serum (FBS) were purchased from Thermo Fisher Scientific (Beijing, China). Other chemicals and reagents used were chromatographic or analytical grade.

Cells

The human colon cancer epithelial (Caco-2) cells were purchased from Cell Resource Center of Peking Union Medical College (Beijing, China).

Animals

Male SD rats weighing 200-240 g were obtained from Animal Center of Xin Jiang Medical University (XinJiang, China). The animals were bred and housed under conventional experimental animal facilities with free access to food and water. The animals were housed in a temperature and humidity controlled room (26 °C, 52 %air humidity) with free access to water for 1 week, before the experiment. In addition, the protocol was approved by the Committee on the Ethics of Animal Experiments of Laboratory Center of Xinjiang Medical University (Permit Numbers: SYXK2011-0004; Urumqi, China).

Preparation of C-CA-R-CPLs

CA-R-CPLs were prepared through the method of ethanol injection as previously described (Zeng *et al.*, 2017). Briefly, CA, R, SPC, HSPC and Cholesterol were dissolved with the ethanol solution. The mixture was completely homogenized through using the ultrasound, then injected into the Phosphate Buffered Saline (PBS, pH = 7.4 and 37°C) and stirred for 45 min via magnetic stirrer and reclaimed. The mixture was sonicate for 5 min by probe sonication for 1 min cycles (1 s working and 2 s

rest) at 400W (Ningbo Xinzhi Bio-tech Co. Ltd., China). Finally, the resulting CA-R-CPLs suspension was extruded via sterile Millipore Express (PES, Millipore, USA) with 0.22 µm pore size.

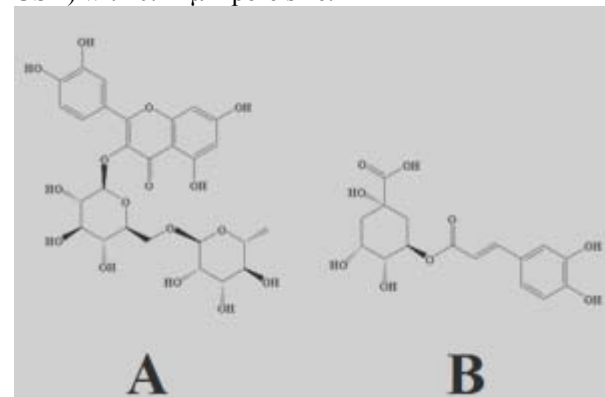


Fig. 1: Chemical structures of A: rutin and B: chlorogenic acid.

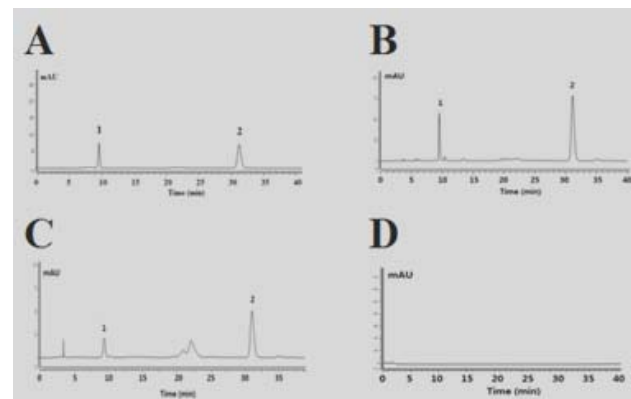


Fig. 2: HPLC chromatograms A. controls; B. CA-R-solution; C. C-CA-R-CPLs; D. negative controls (C-CPLs of blank)(1. chlorogenic acid; 2. Rutin).



Fig. 3: Jugular blood collection in a rat jugular vein catheterization model (conscious).

The chitosan solution was dissolved in 1% acetic acid solution, under continuous magnetic stirring at room temperature for 30 min. The CA-R-CPLs were added to chitosan solution in 1:5 ratios under magnetic stirring for 1 h. The C-CA-R-CPLs were stored in the refrigerator (4°C) overnight before further use.

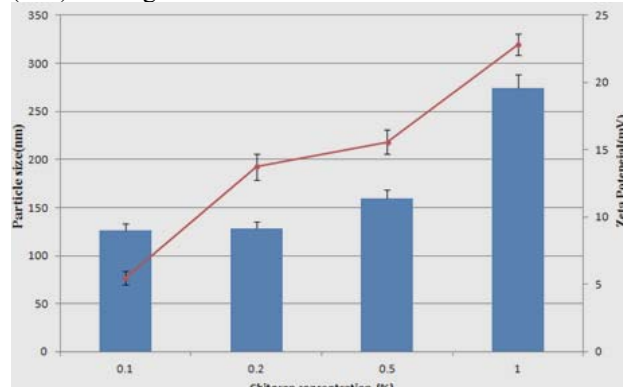


Fig. 4: The particle size and Zeta potential; of different C-CA-R-CPLs.

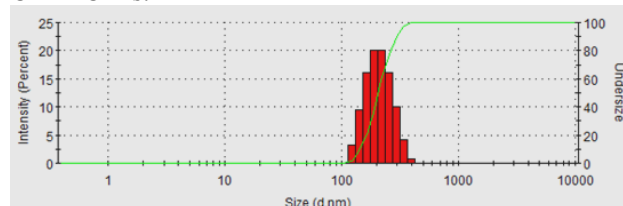


Fig. 5: Particle size values measurements for C-CA-R-CPLs.

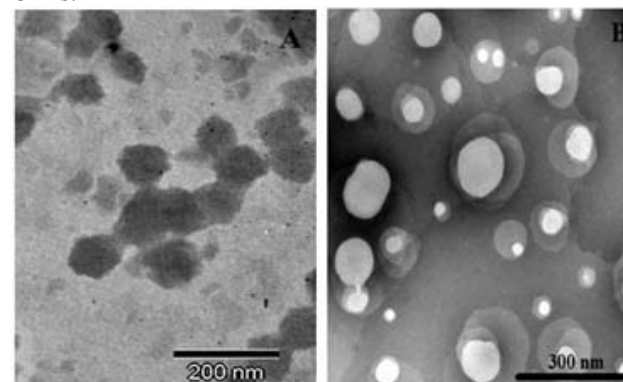


Fig. 6: TEM images of morphology of A (CA-R-CPLs) and B (C-CA-R-CPLs).

Size measurements

The average size and polymey disperse index (PDI) of the CA-R-CPLs and C-CA-R-CPLs were measured via zetasizer (Zetasizer S90, Malvern Instruments, Malvern, UK). Measurements were performed at a scattering angle of 90° and a temperature of 25°C. Prior to their measurements, all of the CA-R-CPLs and C-CA-R-CPLs were previously filtered through 0.22 μm filters to achieve a count rate between 100 and 300 Kcps.

Zeta potential measurements

The zeta potential measurements were performed on a

Zetasizer (Zetasizer S90, Malvern Instruments, Malvern, UK) with the optical modulator operating at 1000 Hz using a dip cell (ZEN1002). To ensure valid measurements, the instrument was calibrated through measurements of the Malvern Zeta Potential Transfer Standard (-50±5 mV). All of the zeta potential measurements were performed at 25°C.

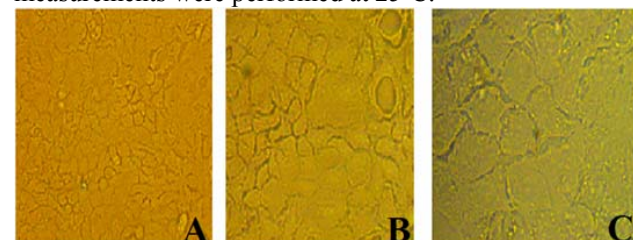


Fig. 7: Integrity of Caco-2 cell monoayers. (A) Morphology of Caco-2 cell monolayers ($\times 10$); (B) Morphology of Caco-2 cell monolayers ($\times 20$); (C) Morphology of Caco-2 cell monolayers ($\times 40$).

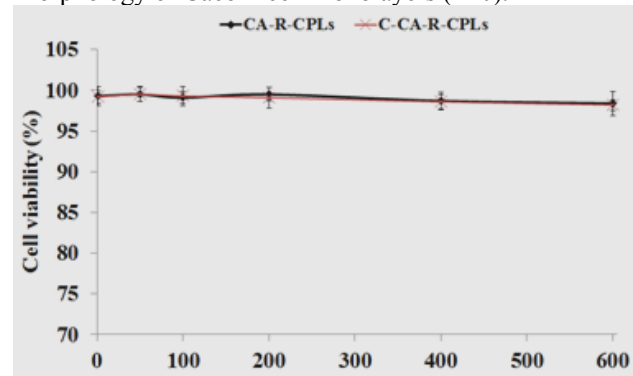


Fig. 8: Cytotoxicity of blank CPLs and blank C-CPLs.

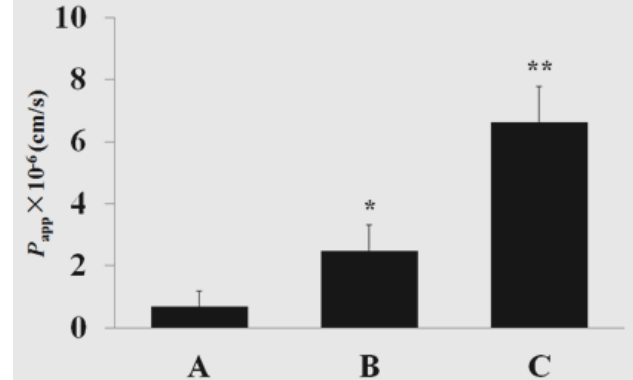


Fig. 9: Permeability values of A (CA-R-solution), B (CA-R-CPLs) and C (C-CA-R-CPLs) (Compared with CA-R-solution, * $P<0.05$, ** $P<0.01$).

Chromatographic system

The High Performance Liquid Chromatography (HPLC) method with DAD detector was developed for the determination of CA and R. The HPLC system consisted of an SCL-10Avp system controller, an LC-10Avp pump, a DGU-14A degasser and a CTO-10Avp column oven (Shimadzu, Kyoto, Japan). A chromatographic C18 column- SPD-10Avp (4.6mm × 250mm, 5μm) was used as analytical column. A binary mobile phase, consisting of

0.4% phosphoric acid (solvent A) and acetonitrile (solvent B), was used at a flow rate of 1.0mL min⁻¹ and with an injection volume of 10 μ L. The gradient elution of the mobile phase was 12% B in 0-15 min, 12-15% B in 16-35 min, 15-12% B in 35-40 min. The column temperature was kept at 35 $^{\circ}$ C. The detection wavelength was set at 353 nm. The 10 μ L of the controls, CA-R-solution, C-CA-R-CPLs and blank C-CPLs were injected respectively. As shown in fig. 2, no interferences were found.

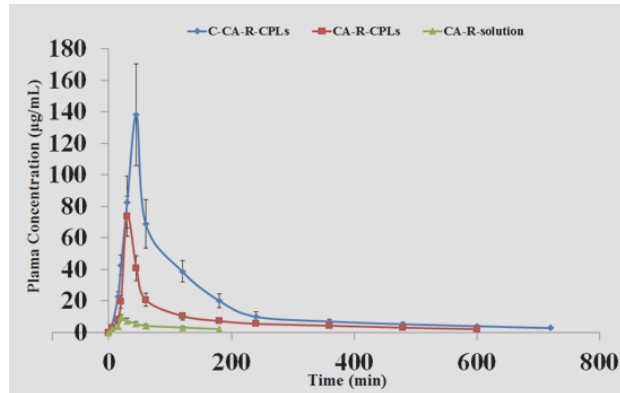


Fig. 10: Mean \pm SD plasma concentration-time profile of CA and R after oral administration of CA-R-solution, CA-R-CPLs and C-CA-R-CPLs at 20 mg/kg dose to rats.

Entrapment efficiency (EE)

EE was determined via gel-filtration method with SephadexG-50 column. In brief, SephadexG-50 solution (10 %, w/v) was prepared in water and was kept aside for 48 h. Cotton was inserted in column (length: 27 cm, inner diameter: 1 cm) and then swollen SephadexG-50 was added carefully to avoid air entrapment in the column. SephadexG-50 was balanced by PBS (pH=7.4).CA-R-CPLs and C-CA-R-CPLs (3 mL) were slowly added into prepared column, flow rate of elution was set at 1 mL/min and volume of elution was 10 times the prepared column volume.

$$EE (\%) = M_{in}/M_{total} \times 100\% \quad (Zeng \text{ et al., 2017})$$

Where M_{in} is the drug amount entrapped, M_{total} is the total drug amount used in the preparation.

Transmission electron microscopy (TEM)

The morphologies of CA-R-CPLs and C-CA-R-CPLs were observed using a TEM (H-600, Hitachi, Japan). After dilution with distilled water, the samples were negatively stained with 2% (w/v) phosphotungstic acid for observation.

CA-R-CPLs and C-CA-R-CPLs stability study

CA-R-CPLs and C-CA-R-CPLs(approximately 50 mL) were stored in plastic centrifuge tube (50 mL) at 4 $^{\circ}$ C in the dark for 6 months. The mean particle size, PDI and EE of CA-R-CPLs and C-CA-R-CPLs were determined at before and after 6 months.

Cell cultures

The Caco-2 cells were maintained in 75 cm² flasks to which 12 mL of Minimum essential medium (MEM), supplemented with 10% (v/v) fetal bovine serum, 1% (v/v) non-essential amino acids, 1% L-glutamine (v/v). The cells were incubated at 37 $^{\circ}$ C in an atmosphere with 95% relative humidity and a CO₂ flow of 5%. The medium was changed every 3 days. When the cell monolayer reached 80% confluence, the cells were detached with a solution of trypsin (0.25 g/L) and EDTA (ethylene diamine tetraacetic acid, 0.22 g/L), and reseeded at a density of 1-1.5 \times 10⁴ cells/cm² (The assays were performed with cultures between passages 22 and 30).

The transport assays were carried out in 12-well plates with polyester membrane inserts (12 mm diameter, pore size 0.4 μ m, Tran swell, Costar Corporation, Beijing, China). In this system the cells are seeded onto the porous membrane of the insert that separates the well into two compartment: Apical (upper) and basolateral (lower). Cells were seeded (8 \times 10⁴ cells/cm²) onto the inserts, with the addition of 0.5 mL of MEM to the apical chamber and 1.5 mL of MEM to the basolateral chamber. The cells were incubated at 37 $^{\circ}$ C, with 5% CO₂ and 95% relative humidity, with a change of medium every 2 days until cell differentiation was reached (16-18 days post-seeding). To evaluate the evolution of the monolayers during cell differentiation in the two-compartment system, the transepithelial electrical resistance (TEER) was measured using a Millicell-ERS voltohmmeter. The cell monolayer was considered completely formed when the resistance reached in the range of 400-600 ohm \cdot cm², cell monolayer was used for transport studies (Fu et al., 2015). Wells with TEER value of >533 ohm \cdot cm².

Permeability studies

The permeation studies of CA-R-solution, CA-R-CPLs and C-CA-R-CPLs were carried out with Caco-2 cells. Culture medium was replaced from each well by Hank's Balanced Salt Solutions (HBSS) in the apical and basolateral side of the well and cell monolayers were subsequently equilibrated for 30 min at 37 $^{\circ}$ C. CA-R-solution, CA-R-CPLs and C-CA-R-CPLs were added into the apical side of the monolayer. The wells were then placed on a shaker at 60 rpm and 37 $^{\circ}$ C for 4 h.

Apparent permeability co-efficient (cm/s) was calculated by the following equation:

$$P_{app} = (dC/dt)/(AC_0)$$

Where, dC/dt = rate of drug permeation (μ g/s), A = Surface area of the insert (cell monolayer) (1.12 cm²), C_0 = Initial concentration of drug in the apical side (μ g/mL). Data reported were arithmetic mean values \pm standard deviation (mean \pm SD). The statistical significance of the differences was performed using an analysis of variance (ANOVA) test and a p value <0.05 or 0.01 was considered significant.

Table 1: Particle size, encapsulation efficiency and zeta potential measurements of CA-R-CPLs and C-CA-R-CPLs (n=6, mean \pm SD)

Formulation	EE ^a (%)	EE ^b (%)	Particle size (nm)	Zeta potential (mV)
“1	82.33 \pm 4.28	85.71 \pm 3.51	116.7 \pm 3.7	-21.8 \pm 1.25
“2	91.3 \pm 2.13	92.6 \pm 2.44	176.7 \pm 2.3	12.61 \pm 1.33

1:CA-R-CPLs; 2: C-CA-R-CPLs; ^a: chlorogenic acid; ^b: rutin**Table 2:** Pharmacokinetic parameters of oral administration of free and formulated drugs in vivo

Parameter	SIHE-solution	SIHECPL	c-SIHECPL
C _{max} (ug/mL)	0.95 \pm 0.35	7.35 \pm 2.12	13.82 \pm 1.24**
T _{max} (min)	15.68 \pm 0.77	25.09 \pm 2.52	31.01 \pm 2.52*
t _{1/2} (min)	9.19 \pm 0.28	12.89 \pm 1.51	14.81 \pm 1.38*
MRT _(0-∞) (min)	18.81 \pm 0.62	27.34 \pm 1.38	43.17 \pm 2.12*
AUC _{0-24 h} (min ug/mL)	41.13 \pm 7.54	328.98 \pm 22.29	609.98 \pm 22.29**
CL (mL/min·kg)	4663.05 \pm 5.64	607.94 \pm 2.23	327.88 \pm 1.65**

Values are expressed as mean \pm SD (n= 6)

* p< 0.05, compared with TFDM-solution

** p< 0.01, compared with TFDM-solution

Evaluation of cytotoxicity

The Caco-2 cells used for the Cell Counting Kit-8 (CCK-8) assay were seeded at a density of 2×10^4 cells/well in 96-well cell culture plates and were pre-incubated for 24 h before sample treatment. Next, the cells were treated with CA-R-CPLs and C-CA-R-CPL sat various lipid concentrations from 1 to 600 μ g/mL in serum-free medium (pH 7.4) for 24 h. The samples were removed, the cells were incubated with 100 μ l of 10% (v/v) CCK-8 and 90% (v/v) MEM for 3 h. The relative cell viability (%) was calculated based on absorbance at 450 nm using a microplate reader. The viabilities of the non-treated control cells were arbitrarily defined as 100%. Relative cell viability (%) was calculated by the following equation:

$$\text{Relative cell viability (\%)} = (\text{OD}_{450, \text{sample}} - \text{OD}_{450, \text{blank}}) / (\text{OD}_{450, \text{control}} - \text{OD}_{450, \text{blank}}) \times 100\%$$

where OD is the optical density at an absorbance of 450 nm.

Oral pharmacokinetics of CA-R-solution, CA-R-CPLs and C-CA-R-CPLs

18 male SD rats (220 \pm 20g) randomly and equally divided into 3 groups. Before the oral administration, all rats were fasted for 12 h, but allowed free access to water. One group of rats was given 20 mg/kg dose of CA-R-solition (2 mg/mL CA and 2mg/mL R, suspended in 0.5% (w/v) CMC-Na aqueous solution) and the others given the same dose of CA-R-CPLs and C-CA-R-CPLs (2mg/mL CA and 2 mg/mL R). The blood samples were collected from the jugular vein at specified intervals (0.01, 5, 15, 30, 45 min, 1,2, 3, 4,6,8, 10 and 12 h after oral administration) (fig. 3). Then the heparinized blood was immediately centrifuged at 3000 rpm for 10 min and treated as described in the “plasma sample preparation” section for further assay.

STATISTICAL ANALYSIS

All the experimental data were expressed as the mean \pm standard error, and a value of P<0.05 was considered statistically significant. Date analyses were performed by using a two-compartmental pharmacokinetic model with the Kinetica 4.4.1 PK/PD analysis (Thermo Electron Corporation, USA). All statistical analyses were analyzed using t-test (paired), and the pharmacokinetic parameter drugs in plasma were achieved.

RESULTS

C-CA-R-CPLs were prepared by the method of ethanol injection and characterized in terms of particle size, encapsulation efficiency and zeta potential. As shown in fig. 4, chitosan solution was used at different concentrations to find the optimum coating level. Zeta potential values did not change whereas, particle size of the formulations were increased as chitosan concentration increase.

Drug loading studies at different chitosan concentrations gave the highest encapsulation efficiency at 0.5% of chitosan concentration (table 1). Therefore, 0.5% of chitosan concentration was selected for coating and this final formulation (C-CA-R-CPLs) has a suitable and excellent particle size and PDI (fig. 5), which was used throughout the present study. Since, CA and R bear negative charge whereas chitosan has positive charge, they possess stronger interaction each other (Ciobanu *et al.*, 2014). There fore, C-CA-R-CPLs may had higher EE compare to uncoated CA-R-CPLs.

As shown in fig. 6, the morphological investigation using TEM revealed nano-formulation sized and spherical

shaped CPL. According to TEM micrographs, C-CA-R-CPLs ranged in size from 100 to 180 nm correlating well with measurement obtained.

The average particle size, PDI of CPLs and the EE of CA-R-CPLs and C-CA-R-CPLs were examined after 6 months of storage at 4°C. An increase of size of CA-R-CPLs from 116.7 ± 3.7 nm to 139.3 ± 2.6 nm and PDI from 0.187 ± 0.033 to 0.227 ± 0.026 and size of C-CA-R-CPLs from 176.7 ± 2.3 nm to 181.5 ± 1.9 nm and PDI from 0.207 ± 0.014 to 0.215 ± 0.018 were observed. However, the EE of CA-R-CPLs and C-CA-R-CPLs determined after 6 months of storage at 4°C were virtually in accordance with those obtained before 6 months suggesting that CA-R-CPLs and C-CA-R-CPLs retain the CA and R constituent during the storage.

The integrity of Caco-2 cell monolayers is shown in fig. 7. With observations under the light microscope, Caco-2 showed a good monolayer formed by 15 day (figs. 7A, B and C). After 5 days of culture, the TEER values of Caco-2 cells increased gradually until reaching maximum ($533/\text{cm}^2$) on 18 day, and these cells did not show any increase of TEER values with time.

The cell viability was calculated as percent of control cells. As shown in fig. 8, CA-R-CPLs and C-CA-R-CPLs showed little or no reduction in cell viability over a wide concentration range from 1 to 600 $\mu\text{g}/\text{mL}$. The cell viability was approximately 100% even at a high concentration (600 $\mu\text{g}/\text{mL}$) of CA-R-CPLs and C-CA-R-CPLs.

The in vitro transport studies in Caco-2 models revealed that the P_{app} of CA-R-CPLs and C-CA-R-CPLs were significantly higher ($P < 0.05$) than P_{app} of CA-R-solution. As shown in fig. 9, nearly 4-fold and 10-fold increase on permeability results of CA and R were obtained from CA-R-CPLs and C-CA-R-CPLs when compared with CA-R-solution.

As shown in fig. 10, the plasma concentration of CA-R-solution increased with time over the 15 min and decrease slowly up to 12 h and the plasma concentration of CA-R-CPLs and C-CA-R-CPLs increased with time over the 30 min and decrease slowly up to 12 h. Meanwhile, in table 2, the relevant pharmacokinetic parameters of CA-R-solution, CA-R-CPLs and C-CA-R-CPLs were listed. The C_{max} , $AUC_{0-12\text{h}}$ and CL of CA-R-solution, CA-R-CPLs and C-CA-R-CPLs showed a highly obvious difference ($P < 0.05$). The C-CA-R-CPLs of T_{max} and $t_{1/2}$ extended to 31.01 ± 2.52 min and 14.81 ± 1.38 min ($P < 0.05$), respectively. The C_{max} in CA-R-solution was 0.95 ± 0.35 $\mu\text{g}/\text{mL}$, which was different from that in the CA-R-CPLs of 7.35 ± 2.12 $\mu\text{g}/\text{mL}$ and C-CA-R-CPLs of 13.82 ± 1.24 $\mu\text{g}/\text{mL}$ ($P < 0.01$). The relative oral bioavailability of the encapsulated CA and R were 799.85 % (CA-R-CPLs) and

1454.74 % (C-CA-R-CPLs) as compared with the CA-R-solution, which was obviously enhanced ($P < 0.01$).

DISCUSSION

In recent years, Caco-2 cell model has been universally applied to assess absorption of drug molecules and transmembrane transport of different liposomes through the intestinal mucosa. But it cannot response the complete physiology of the intestine, which resulting in inappropriate in vitro/in vivo correlations. In recent years, a novel intestinal in vitro triple culture permeability model including HT29-MTX cells, M cells and Parallel artificial membrane permeability assay (PAMPA) was developed (Hermida *et al.*, 2011). It was found that mucus strongly impacts mobility of nanoformulations and that specialized M cells are involved in particulate uptake (Maet *et al.*, 2013). Nanoformulations uptake mainly depend on size and which was strongly impacted by the mucus layer. In addition, nanoformulations were able to penetrate the intestinal barrier mainly via specialized M cells (Singhet *et al.*, 2014). And compared to single Caco-2 cell monolayers, the higher uptake amounts are attributed to the presence of M cells, which are barely covered with mucus and play a significant role in nanoformulations entry of the intestinal epithelium (Zhang *et al.*, 2015).

Currently, C-CPLs have been commonly used for oral drug delivery to improve the oral bioavailability of some drugs that are not easily absorbed. Because of the amphiphilic nature of CPLs, these vesicular carriers, which are composed of SPC and HSPC, are able to carry hydrophilic or hydrophobic drug molecules. Just like the fig. 10 shown, a pharmacokinetically well defined plasma concentration profile was observed. One of the major causes for enhancing oral bioavailability might be that C-CPLs could protect drugs from degrading or adsorbing in the stomach after oral administration (Lila *et al.*, 2009). In addition, the majority of drugs stays inside of carriers of CPLs and thus drugs itself may not have a chance to contact esophagus and get higher oral bioavailability (Liuet *et al.*, 2015; Zheng *et al.*, 2014). Meanwhile, CPLs were composed of the different phospholipid bilayers (SPC and HSPC), resulting in improving the membrane permeability and cellular absorption. Also, biocompatible stuffs have been used for surface layers of CPLs to extend the residence time in intestine (Zhu *et al.*, 2015; Kheirolumoom *et al.*, 2013). And the CPLs with cholesterol would also enhance stability of CPLs in vivo (Li *et al.*, 2015). Because of the drug had to pass through the phospholipid bilayer, which made the drug release slowly and CPLs were extended residence time in intestine might conduce to improve the drug absorption (Zeng *et al.*, 2016). In addition, chitosan incorporate CA-R-CPLs made it more difficult to release the drug. Thereby the chitosan increased the prolonged time of CA and R *in vivo* (Shi *et al.*, 2015).

Overall, according to our research about the oral administration, the relative oral bioavailability of C-CA-R-CPLs had an outstanding improvement in comparison with the CA-R-solution, with almost 14-fold increase in relative oral bioavailability. Therefore, the extended circulation time and higher AUC of C-CA-R-CPLs will contribute to better therapeutic efficacy on liver disease.

CONCLUSION

CA and R are compounds of poorly soluble and low oral bioavailability were successfully prepared of C-CA-R-CPLs by the method of ethanol injection. According to the physicochemical properties, which with high EE, small average particle size, well suited PDI. The final formulation was able to potentially increase uptake of CA and R through in-vitro transport studies (Caco-2 models). And according to the Pharmacokinetics studies, C-CA-R-CPLs could be effective to enhance bioavailability of CA and R after oral administration *in vivo*. The result has indicated that the Caco-2 permeability and *in vivo* pharmacokinetics results have a certain correlation and similar variation trends to the oral absorption of C-CA-R-CPLs, but have a certain degree of deviation in values. In addition, the CA-R-CPLs and C-CA-R-CPLs were also stable after 6 months of storage at 4°C. Therefore, the novel nano-formulation (c-CPLs) could be a promising oral drug deliver carrier for low water solubility and poorly absorbed drugs to enhance oral bioavailability of CA and R.

ACKNOWLEDGMENTS

This study was supported by the National Natural Science Foundation of China (H0203) and Plan for Supporting Xinjiang through Science and Technology in Xinjiang Uygur Autonomous Region (201591149).

REFERENCES

Byambaragchaa M, Dela Cruz J, Kh A and Hwang SG (2014). Anticancer potential of an ethanol extract of *Saussurea involucrata* against hepatic cancer cells in vitro. *Asian Pac. J. Cancer Prev.*, **15**: 7527-7532.

Caddeo C, Pons R, Carbone C, Fernández-Busquets X, Cardia MC, Maccioni AM, Fadda AM and Manconi M (2017). Physico-chemical characterization of succinyl chitosan-stabilized liposomes for the oral co-delivery of quercetin and resveratrol. *Carbohydr. Polym.*, **157**: 1853-1861.

Chik WI, Zhu L, Fan LL, Yi T, Zhu GY, Gou XJ, Tang YN, Xu J, Yeung WP, Zhao ZZ, Yu ZL and Chen HB (2015). *Saussurea involucrata*: A review of the botany, phytochemistry and ethnopharmacology of a rare traditional herb medicine. *J. Ethnopharmacol.*, **172**: 44-60.

Ciobanu BC, Cadinoiu AN, Popa M, Desbrieres J and Peptu CA (2014). Modulated release from liposomes entrapped in chitosan/gelatin hydrogels. *Mater. Sci. Eng. C Mater. Biol. Appl.*, **43**: 383-391.

Fu Q, Wang H, Xia M, Deng B, Shen H, Ji G, Li G and Xie Y (2015). The effect of phytic acid on tight junctions in the human intestinal Caco-2 cell line and its mechanism. *Eur. J. Pharm. Sci.*, **88**: 1-8.

Hermida LG, Roig A, Bregni C, Sabés-Xamaní M and Barnadas-Rodríguez R (2011). Preparation and characterization of iron-containing liposomes: Their effect on soluble iron uptake by Caco-2 cells. *J. Liposome Res.*, **21**: 203-212.

Huang A, Su Z, Li S, Sun M, Xiao Y, Ping Q and Deng Y (2014). Oral absorption enhancement of salmon calcitonin by using both N-trimethyl chitosan chloride and oligoarginines-modified liposomes as the carriers. *Drug Deliv.*, **21**: 388-396.

Kheirolooom A, Lai CY, Tam SM, Mahakian LM, Ingham ES, Watson KD and Ferrara KW (2013). Complete regression of local cancer using temperature-sensitive liposomes combined with ultrasound-mediated hyperthermia. *J. Control Release*, **172**: 266-273.

Klemetsrud T, Kjønnsken AL, Hiorth M, Jacobsen J and Smistad G (2016). Polymer coated liposomes for use in the oral cavity - a study of the in vitro toxicity, effect on cell permeability and interaction with mucin. *J. Liposome Res.*, **28**: 1-12.

Li Y, Liu R, Yang J, Shi Y, Ma G, Zhang Z and Zhang X (2015). Enhanced retention and anti-tumor efficacy of liposomes by changing their cellular uptake and pharmacokinetics behavior. *Biomaterials*, **41**: 1-14.

Lila AS, Kizuki S, Doi Y, Suzuki T, Ishida T and Kiwada H (2009). Oxaliplatin encapsulated in PEG-coated cationic liposomes induces significant tumor growth suppression via a dual-targeting approach in a murine solid tumor model. *J. Control Release*, **137**: 8-14.

Liou CJ, Wu SJ, Chen LC, Yeh KW, Chen CY and Huang WC (2017). Acacetin from traditionally used *Saussurea involucrata* Kar. et Kir. suppressed adipogenesis in 3T3-L1 adipocytes and attenuated lipid accumulation in obese mice. *Front Pharmacol.*, **8**: 589.

Liu C, Shi J, Dai Q, Yin X, Zhang X and Zheng A (2015). In-vitro and *in-vivo* evaluation of ciprofloxacin liposomes for pulmonary administration. *Drug Dev. Ind. Pharm.*, **41**: 272-278.

Ma J, Guan R, Shen H, Lu F, Xiao C, Liu M and Kang T (2013). Comparison of anticancer activity between lactoferrin nanoliposome and lactoferrin in Caco-2 cells *in vitro*. *Food Chem. Toxicol.*, **59**: 72-77.

Park SN, Jo NR and Jeon SH (2014). *In-vitro* digestion of curcumin loaded chitosan-coated liposomes. *Colloids Surf B Biointerfaces*, **S0927-7765**: 30788-30789.

Shi LL, Cao Y, Zhu XY, Cui JH and Cao QR (2015). Optimization of process variables of zanamivir-loaded solid lipid nanoparticles and the prediction of their

cellular transport in Caco-2 cell model. *Int. J. Pharm.*, **478**: 60-69.

Singh RS, Michel D, Das U, Dimmock JR and Alcorn J (2014). Cytotoxic 1,5-diaryl-3-oxo-1,5-pentadienes: An assessment and comparison of membrane permeability using Caco-2 and MDCK monolayers. *Bioorg. Med. Chem. Lett.*, **24**: 199-202.

Su KY, Yu CY, Chen YW, Huang YT, Chen CT, Wu HF and Chen YL (2014). Rutin, a flavonoid and principal component of saussurea in volucrata, attenuates physical fatigue in a forced swimming mouse model. *Int. J. Med. Sci.*, **11**: 528-537.

Tejera-Garcia R, Parkkila P, Zamotin V and Kinnunen PK (2014). Principles of rational design of thermally targeted liposomes for local drug delivery. *Nanomedicine*, **10**: 1243-1252.

Vanić Ž, Hafner A, Bego M and Škalko-Basnet N (2013). Characterization of various deformable liposomes with metronidazole. *Drug Dev. Ind. Pharm.*, **39**: 481-488.

Wang M, Liu M, Xie T, Zhang BF and Gao XL (2017). Chitosan-modified cholesterol-free liposomes for improving the oral bioavailability of progesterone. *Colloids Surf B Biointerfaces*, **159**: 580-585.

Wieber A, Seizer T and Kreuter J (2011). Characterization and stability studies of a hydrophilic decapeptide in different adjuvant drug delivery systems: A comparative study of PLGA nanoparticles versus chitosan-dextran sulphate microparticles versus DOTAP-liposomes. *Int. J. Pharm.*, **421**: 151-159.

Xie Q, Shen KN, Hao X, Nam PN, Nqoc Hieu BT, Chen CH, Zhu C, Lin YC and Hsiao CD (2017). The complete chloroplast genome of Tianshan Snow Lotus (Saussureainvolucrata), a famous traditional Chinese medicinal plant of the family Asteraceae. *Mitochondrial DNA A DNA Mapp. Seq. Anal.*, **28**: 294-295.

Yao L, Zhao Q, Xiao J, Sun J, Yuan X, Zhao B, Su H and Niu S (2012). Composition and antioxidant activity of the polysaccharides from cultivated Saussurea involucrata. *Int. J. Biol. Macromol.*, **50**: 849-853.

Zeng C, Jiang W, Tan M, Xing J and He C (2016). Improved oral bioavailability of total flavonoids of *Dracocephalum moldavica* via composite phospholipid liposomes: preparation, *in vitro* drug release and pharmacokinetics in rats. *Pharmacogn Mag.*, **12**: 313-318.

Zeng C, Jiang W, Tan M, Yang X, He, Huang W and Xing J (2016). Optimization of the process variables of tiliatin-loaded composite phospholipid liposomes based on response surface-central composite design and pharmacokinetic study. *Eur. J. Pharm. Sci.*, **85**: 123-131.

Zeng C, Xue G, Yang X, He C, Huang W and Xing J (2017). Enhancing the *in vitro* release of total flavonoids extract from *Dracocephalum moldavica* composite phosphor lipid liposomes optimized by response surface methodology. *Pak. J. Pharm. Sci.*, **30**: 1225-1232.

Zhang Y, Zhang H, Wang F, Yang D, Ding K and Fan J (2015). The ethanol extract of *Eucommia ulmoides* Oliv. Leaves inhibits disaccharidase and glucose transport in Caco-2 cells. *J. Ethnopharmacol.*, **163**: 99-105.

Zheng Y (2014). Editorial: Novel formulation strategies for poorly water-soluble drugs and herbal medicines. *Curr. Pharm. Des.*, **20**: 301-302.

Zhou Y, Ning Q, Yu DN, Li WG and Deng J (2014). Improved oral bioavailability of breviscapine via a Pluronic P85-modified liposomal delivery system. *J Pharm. Pharmacol.*, **66**: 903-911.

Zhu Y, Wang M, Zhang J, Peng W, Firempong CK, Deng W, Wang Q, Wang S, Shi F, Yu J, Xu X, Zhang W (2015). Improved oral bioavailability of capsaicin via liposomal nano formulation: Preparation, *in vitro* drug release and pharmacokinetics in rats. *Arch pharm. Res.*, **38**: 512-521.